SPECTRAL AND INTEGRATED ABSORPTION OF SOLAR RADIATION IN BROKEN CLOUDS

G.A. Titov and T.B. Zhuravleva

Institute of Atmospheric Optics,
Siberian Branch of the Russian Academy of Sciences, Tomsk
Received April 18, 1995

In the paper, we investigate the mean spectral and integrated absorption of solar radiation in broken clouds. It is shown that the random geometry of a cloud field has strong influence on the spectral radiation absorption in clouds. Its effect is less important for the integrated absorption, while becoming stronger with increasing cloud extinction coefficient and underlying surface albedo, as well as at intermediate cloud fractions. This must be kept in mind when developing radiation codes of general circulation models.

It is recognized now that a plane-parallel atmospheric model describes unsatisfactorily the radiative transfer through broken clouds, and hence the radiation codes of general circulation models (GCMs) must be refined. However, before introducing one or another change in GCMs, of necessity is to investigate the dependence of the radiative characteristics on the random geometry of a cloud field. Such studies for the mean flux of downwelling and upwelling solar radiation in the visible and near-IR spectral ranges were performed in Refs. 1–4.

In the present paper, we investigate the mean spectral and integrated absorption of solar radiation by broken clouds (hereafter, the term "mean" will be omitted for convenience). To evaluate the potential effect of the stochastic geometry, we will compare the absorption by cumulus ($0.5 \le \gamma \le 2$) with that by equivalent stratus ($\gamma \ll 1$). Here, $\gamma = H/D$, H is the cloud layer thickness, and D is the characteristic horizontal cloud size. The equivalent stratus differ from cumulus only in the ratio γ, all other parameters being equal. The spectral absorption $A(\lambda)$ in stratus partially covering the sky can be calculated from the formula

$$A(\lambda) = N\,A_{\rm lay}(\lambda) + (1 - N)\,A_{\rm cle}(\lambda)\ ,$$

where N is the cloud fraction, $A_{\rm cle}(\lambda)$ and $A_{\rm lay}(\lambda)$ are the values of spectral absorption in clear sky and plane-parallel cloud layer, respectively. Obviously, analogous formula is applied to calculate the integrated absorption.

Model of the atmosphere and methods of spectral flux calculations in the near-IR were described in detail in Refs. 1–5. It should be only recalled that the atmosphere is assumed to extend vertically to 16 km, clouds are in the 1–1.5 km layer, and the absorption by water vapor and carbon dioxide is considered. It is assumed that unitary flux of solar radiation is incident on the top of the atmosphere in the direction $\omega_\oplus = (\xi_\oplus, \varphi_\oplus)$, with $\xi_\oplus$ and $\varphi_\oplus$ being the solar zenith and azimuth angles. Absolute values of spectral absorption can be obtained by multiplying our results by $\pi S_\lambda \cos\xi_\oplus$, with πS_λ being the spectral solar constant.

Since the optical thickness of the atmospheric aerosol is much smaller than that of clouds, the difference between absorption in cumulus and stratus will be primarily due to multiple scattering in clouds. So we restrict ourselves to a discussion of the absorption by a cloud layer. In addition, we can neglect the scattering of radiation in the atmospheric layer above the cloud due to its small optical thickness and hence the dependence of solar radiation incident on the cloud top on the cloud type.

SPECTRAL ABSORPTION

As is well known, the absorption by cloud particles (water droplets) increases with the increase of the fraction of diffuse radiation and the mean multiplicity of scattering, as well as with the decrease of the single scattering albedo w_λ. From the above definition of equivalent stratus it follows that only the first two of these parameters depend on the cloud type. At fixed pressure, temperature, and gas concentration, the absorption by atmospheric gases is determined by the photon mean free path in clouds. We begin the discussion of calculated results with the simplest case in which the albedo of the underlying surface A_s is zero, which approximately corresponds to the albedo of the ocean.

Radiation may leave cumulus through their sides, so that the mean multiplicity of scattering and the photon mean free path in cumulus are less than in stratus. When the sun is in zenith, the fraction of diffuse radiation is the same for both cloud types; thus, the absorption in stratus $A_{\rm St}(\lambda)$ exceeds the absorption in cumulus $A_{\rm Cu}(\lambda)$ (Fig. 1).

0235-6880/95/10 767-05 $02.00

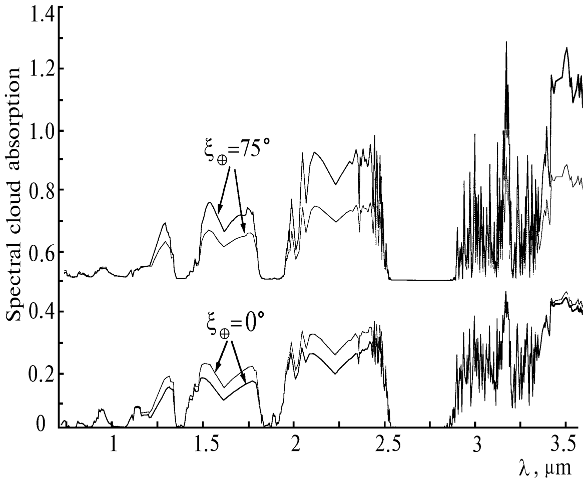

FIG. 1. Dependence of spectral absorption in cumulus (solid curves) and stratus (dotted curves) on the solar zenith angle with $N = 0.5$, $\sigma_{0.71\ \mu m} = 30\ km^{-1}$, $D = 0.25$ km, *and* $A_s = 0$. *For vivid presentation, values of cloud absorption at* $\xi_\oplus = 75°$ *are exaggerated by* 0.5.

Except for $\xi_\oplus > 80°$, the fraction of diffuse radiation in stratus depends very weakly on $\xi_\oplus$, while increases rapidly with $\xi_\oplus$ in cumulus. In cumulus, this leads to the increase of the absorption, which may compensate for the decrease of the mean multiplicity of scattering and photon mean free path. Thus, there are two opposite effects whose net sign can be determined by separation of the spectral absorption of different multiplicity. Obviously, the nth term of the expansion is proportional to $w_\lambda^{n-1}(1 - w_\lambda)$. When the single scattering albedo approaches unity, a pronounced contribution to the spectral absorption will come from higher-order scattering. Lower-order scattering is more important in cumulus, while the higher-order scattering is more important in stratus. For wavelengths $\lambda \le 1.2$ μm, water droplets absorb weakly ($w_\lambda \ge 0.999$). For such values of w_λ, the increasing diffuse fraction may not always compensate for the decreasing mean scattering order and photon mean free path; as a result, the spectral absorption in cumulus is less than that in stratus even at large solar zenith angles (Fig. 1). The situation is reverse for $\lambda \ge 1.2$ μm, when water droplets absorb strongly ($0.485 \le w_\lambda \le 0.999$).

Let us discuss the dependence of the spectral absorption on the solar zenith angle for each cloud type. To this end, we represent the results shown in Fig. 1 in another form shown in Fig. 2.

As the solar zenith angle $\xi_\oplus$ increases, the solar radiation incident on the cloud top decreases due to the gaseous absorption and aerosol extinction; in addition, cloud albedo increases, and the mean scattering order and mean path length of reflected photons decrease. For these reasons, the absorption in stratus decreases as $\xi_\oplus$ increases.

The pattern is more complicated in cumulus. For moderate values of the gaseous absorption, the increasing fraction of diffuse radiation dominates over the other effects mentioned above, and the absorption in cumulus increases. In the case of strong absorption, the dependence is reverse.

Let us suppose now that the underlying surface reflects according to Lambert's law and has the albedo $A_s > 0$. This surface can be considered as a diffuse source whose power is proportional to $A_sQ(\lambda)$, where $Q(\lambda)$ is the spectral transmittance at the surface level. Obviously, only in case of weak to moderate droplet and gaseous absorption, as well as with the problem parameters that provide sufficiently large $A_sQ(\lambda)$, the radiation reflected from the underlying surface will noticeably affect the spectral absorption in clouds. Radiation reflected from the underlying surface may interact with the sides of numerous cumulus, i.e., may be scattered and absorbed. Quantitatively, this means that the fraction of radiation transmitted through the gaps between the clouds will be much less in cumulus than in stratus. As a consequence, cumulus absorbs larger fraction of radiation reflected from the underlying surface than the stratus does.

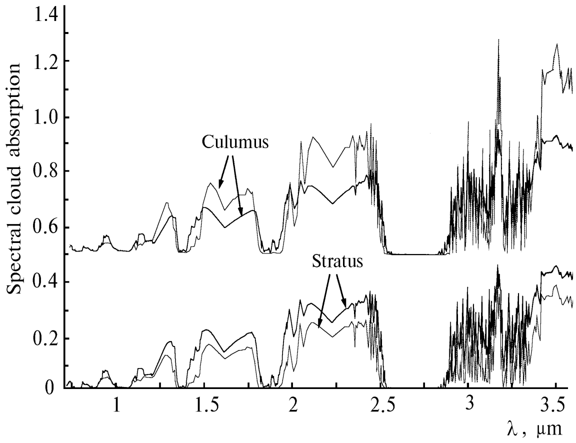

FIG. 2. Same as in Fig. 1: $\xi_\oplus = 0°$ *(solid curves) and* 75° *(dotted curves). For vivid presentation, the values of the absorption in cumulus are exaggerated by* 0.5.

The aforesaid is confirmed by the results of our calculations of the spectral absorption shown in Fig. 3. For wavelengths $\lambda \ge 1.2$ μm, when the sun is in zenith and $A_s = 0.8$ (the albedo of a snow cover), the absorption in cumulus exceeds that in stratus, in contrast to the case of $A_s = 0$ (see Fig. 1). In addition to the above reason, the increment to the absorption in cumulus is sufficiently large because the transmittance of cumulus $Q(\lambda)$ is higher than that of stratus.

At large solar zenith angles ($\xi_\oplus = 75°$), the inequality $A_{Cu}(\lambda) \ge A_{St}(\lambda)$ holds true for $A_s = 0.8$, as in the case of $A_s = 0$ (cf. Fig. 1). Increasing surface albedo results in the insignificant increase of the absorption in cumulus, since the fraction of unscattered radiation and hence the transmittance $Q(\lambda)$ decrease with increasing $\xi_\oplus$. This diminishes the power of the diffuse source which is considered to be the underlying surface, and the increment to the absorption in cumulus is not as large as at $\xi_\oplus = 0°$. In the case of stratus partially covering the sky, radiation reflected from the underlying surface passes through the gaps between the clouds and has little effect on the spectral absorption $A_{St}(\lambda)$ when A_s is varied.

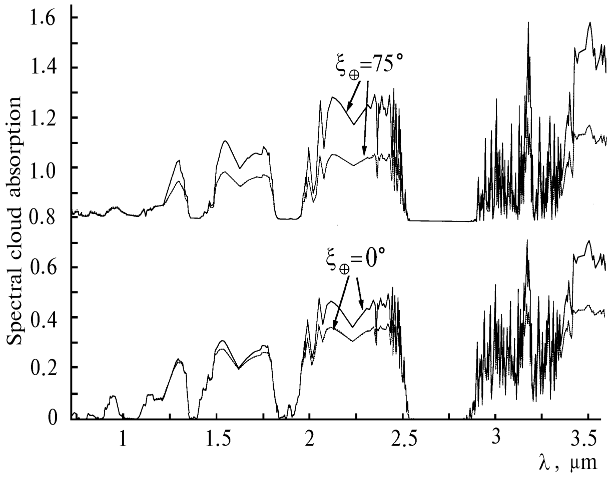

FIG. 3. Same as in Fig. 1 but for $A_s = 0.8$. *For vivid presentation, the values of the cloud absorption at* $\xi_\oplus = 75°$ *are exaggerated by* 0.8.

In modeling of formation and dynamics of cloud systems, account must be taken of the specific features of thermal regime within the cloud layer. The characteristic being most widely employed in the cloud thermal regime treatment is the time rate of change of the radiant temperature due to short-wave radiation absorption, $(\partial T/\partial t)$. In this context, of interest are salient features of vertical distribution of solar absorption across the cloud layer.

Now let us divide the cloud layer into M sublayers with boundaries $z_i = \text{const}$, $i = 1, ..., M, M + 1$, where z_1 and z_{M+1} are the lower and upper boundaries of the cloud layer, respectively. Let $A(\lambda, z_i, z_{i+1})$ denote the mean absorption in the layer (z_i, z_{i+1}). Then the mean absorption in the cloud layer $A(\lambda, z_1, z_{M+1})$ is given by the relation

$$A(\lambda, z_1, z_{M+1}) = \sum_{i=1}^{M} A(\lambda, z_i, z_{i+1}) .$$

In practice, a variety of parameters are used to describe the absorption within the cloud layer[6-8]; we choose the probability density distribution of absorption across the cloud layer $p_i(\lambda, z)$ defined as

$$p_i(\lambda, z) = \frac{A(\lambda, z_i, z_{i+1})}{A(\lambda, z_1, z_{M+1})\,(z_{i+1} - z_i)} ,$$

together with the parameter $P_i(\lambda, z)$ characterizing the contribution of the ith layer to the total cloud absorption given by the formula

$$P_i(\lambda, z) = \frac{A(\lambda, z_i, z_{i+1})}{A(\lambda, z_1, z_{M+1})}\, 100\% .$$

Analogous characteristics were used, e.g., in Ref. 6.

In our computations, cloud sublayers of different thickness were used: 0.05 km thick between 1.0 and 1.2 km and 0.02 km thick between 1.2 and 1.5 km.

Shown in Fig. 4 is the probability density distribution of solar radiation absorption for two wavelengths, $\lambda = 1.426$ μm with moderate absorption by cloud droplets ($w_\lambda = 0.967$) and atmospheric gases (Fig. 4*a*), and $\lambda = 2.224$ μm with moderate absorption by cloud droplets ($w_\lambda = 0.973$) and weak absorption by atmospheric gases (Fig. 4*b*). For $A_s = 0$, the vertical profile of $p_i(\lambda, z)$ depends weakly on the wavelength and has the following features: (*a*) the density distribution of absorption is maximum at the top of the cloud layer ($z \approx z_1 + 0.9H$); and (*b*) near the upper cloud boundary ($z_1 + 0.8H \le z \le z_1 + H$), cumulus absorbs more intensively than stratus: $p_{i,Cu}(\lambda, z) \ge p_{i,St}(\lambda, z)$.

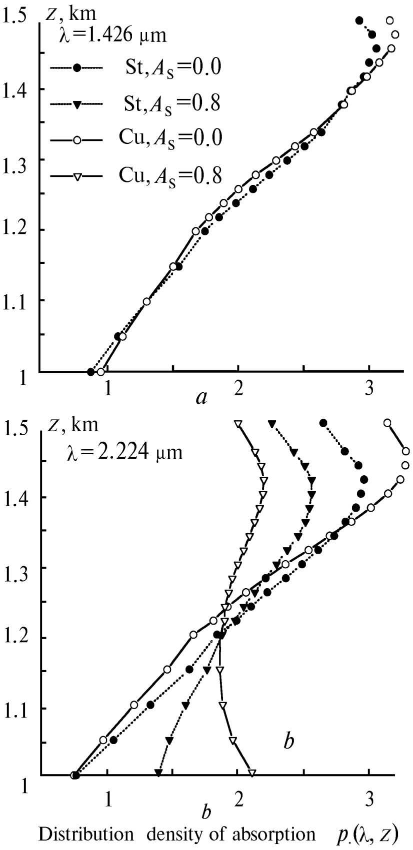

FIG. 4. Vertical distribution density $p_i(\lambda, z)$ *of solar radiation absorption within the cloud layer for wavelengths* $\lambda = 1.426$ *(a) and* 2.224 μm *(b) with* $N = 0.5$, $\sigma_{0.71\mu m} = 30\ \text{km}^{-1}$, *and* $D = 0.25$ km *at* $\xi_\oplus = 0°$.

With increase of the underlying surface albedo for weak gaseous absorption ($\lambda = 2.224$ μm), the vertical profiles $p_i(\lambda, z)$ differ qualitatively in cumulus and stratus. In particular, at $\xi_\oplus = 0°$ the transmittance at the surface level is sufficiently high, so that surface-reflected radiation can significantly contribute to the cloud absorption, thereby causing the occurrence of the secondary maximum in $p_i(\lambda, z)$ near the cumulus bottom. As atmospheric gaseous absorption increases ($\lambda = 1.426$ μm), $Q(\lambda)$ sharply decreases, and the increment to the absorption due to the surface-reflected radiation becomes insignificant. For moderate to strong gaseous absorption, the probability density distribution of solar radiation absorption changes insignificantly both in cumulus and stratus in comparison with $A_s = 0$.

Table I presents the vertical distribution $P_i(\lambda, z)$. When $A_s = 0$, for weak and moderate gaseous absorption, contribution of different parts of the cloud layer $P_i(\lambda, z)$ depends weakly on the cloud type: the upper part of the cloud layer absorbs ~30%, while the lower part – nearly 10% of solar radiation. For higher surface albedos, $P_i(\lambda, z)$ profile changes insignificantly with cloud type for moderate absorption by atmospheric gases, while it depends strongly on the cloud type for weak gaseous absorption. Thus, in cumulus, the upper and lower parts of the cloud layer become equally absorptive, both absorbing ~20% of solar radiation. In stratus, greatest contribution comes from the upper part of the cloud layer as before, but the difference between $P_i(\lambda, z)$ values near the upper and lower boundaries reduces to 10%.

TABLE I. Vertical distribution $P_i(\lambda, z)$ (%), with $\sigma_{0.71\mu m} = 30$ km^{-1}, $N = 0.5$, and $D = 0.25$ km, at $\xi_\oplus = 0°$.

Layer, km	λ = 1.426 μm				λ = 2.224 μm			
	$A_s = 0$		$A_s = 0.8$		$A_s = 0$		$A_s = 0.8$	
	Cu	St	Cu	St	Cu	St	Cu	St
1.48–1.5	6.29	5.85	5.67	5.63	6.25	5.26	3.99	4.51
1.46–1.48	6.36	6.03	5.77	5.8	6.52	5.61	4.24	4.83
1.44–1.46	6.3	6.11	5.73	5.87	6.52	5.79	4.35	5.01
1.42–1.44	6.13	5.97	5.6	5.79	6.41	5.87	4.38	5.11
1.4–1.42	5.96	5.89	5.47	5.72	6.25	5.85	4.35	5.12
1.4–1.5	31.04	29.85	28.24	28.81	31.96	28.38	21.31	24.58
1.3–1.4	25.73	26.19	24.13	25.6	26.83	27.04	20.8	24.29
1.2–1.3	18.96	19.87	18.86	19.82	19.25	20.99	19.04	20.4
1.1–1.2	13.97	14.19	15.29	14.78	13.21	14.72	18.62	16.72
1.0–1.1	10.3	9.9	13.48	10.99	8.87	8.99	20.23	14.01

INTEGRATED ABSORPTION

By integrated absorption we mean the quantity

$$A = \frac{\int_{0.7\ \mu m}^{3.6\ \mu m} \pi S_\lambda A(\lambda) \cos\xi_\oplus d\lambda}{\pi S \cos\xi_\oplus} 100\% ,$$

where $\pi S = 1353$ Wm^{-2} is the integrated solar constant. Major contributors to the integrated absorption are those spectral intervals in which $A(\lambda)$ and πS_λ are sufficiently large. Clearly, variations of the integrated absorption are fully determined by the dependence of the spectral absorption on the problem parameters, so some obvious cases will be without comments. Recall that the wavelength interval 0.7–1.2 μm comprises ≈ 30% of the solar radiation flux incident on the top of the atmosphere, while the 1.2–2 μm and 2–4 μm wavelength intervals comprise ≈15% and 5%, respectively.[9]

As the solar zenith angle increases, the integrated cloud absorption A_{cl} decreases in stratus and slightly increases in cumulus (Fig. 5). The latter is due to the fact that the spectral absorption in cumulus, $A_{Cu}(\lambda)$, may increase or decrease with increase of $\xi_\oplus$ (Fig. 2); thus, A_{cl} consists of two terms that are reverse functions of $\xi_\oplus$.

The term which decreases with increasing solar zenith angle is formed at wavelengths $\lambda \le 2.25$, where πS_λ is relatively large. So this term is sufficiently large, and thus A_{cl} increases insignificantly with increasing solar zenith angle. At the same time, the increase of the solar zenith angle results in the significant increase of the integrated absorption in the abovecloud atmosphere, and the total integrated atmospheric absorption increases both in cumulus and stratus (see Fig. 5).

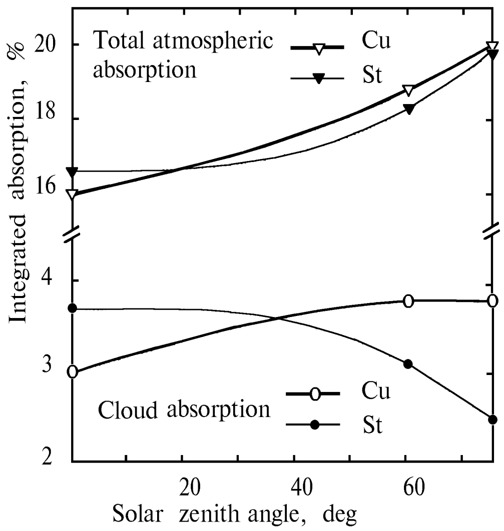

FIG. 5. Influence of the solar zenith angle on the integrated absorption with $N = 0.5$, $\sigma_{0.71\mu m} = 30$ km^{-1}, $D = 0.25$ km, and $A_s = 0$.

The finite horizontal size of cumulus is responsible for the nonlinear (in contrast to stratus) dependence of the integrated absorption on the cloud fraction N (Fig. 6). The maximum difference between the integrated absorption in cumulus and stratus occurs at intermediate cloud fractions. Its value increases with surface albedo.

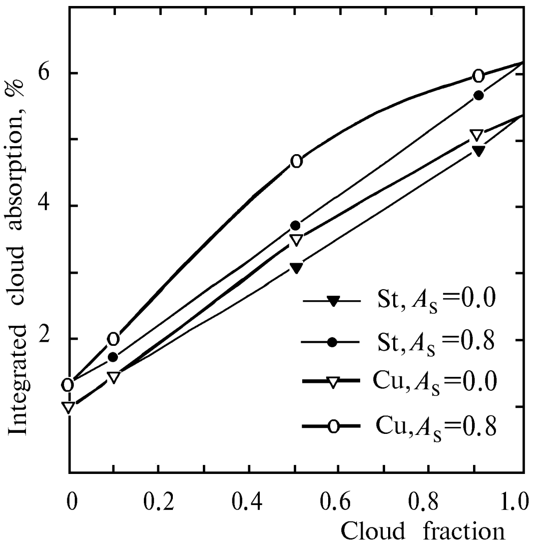

FIG. 6. Dependence of the integrated absorption on the cloud fraction with $\sigma_{0.71\mu m} = 30\ km^{-1}$ *and* $D = 1.0$ km *at* $\xi_{\oplus} = 60°$.

As cloud optical thickness increases, the relative contribution of cloud sides and cloud radiative interaction also increases. As a result, with increasing cloud extinction coefficient σ (at fixed cloud geometric thickness) the difference between the absorption in cumulus and stratus also increases (Fig. 7).

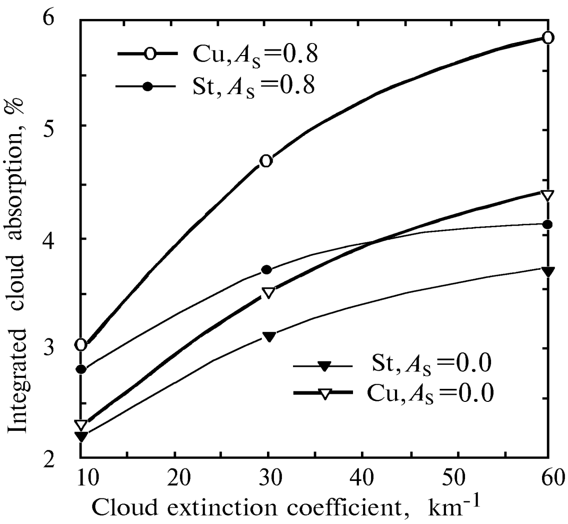

FIG. 7. Integrated cloud absorption with $N = 0.5$ *and* $D = 1.0$ km *at* $\xi_{\oplus} = 60°$ *as function of the cloud extinction coefficient.*

CONCLUSION

Our results clearly demonstrate that the stochastic geometry of cloud fields significantly affects the spectral solar radiation absorption in clouds. Its impact on the integrated absorption is not so strong; however, it strengthens with increasing cloud extinction coefficient and surface albedo as well as at intermediate cloud fractions. This indicates that GCM radiation codes should be appropriately refined.

At present, we have a large body of calculated results for spectral and integrated flux of upwelling and downwelling solar radiation and radiation absorption. These data can be considered as a numerical radiation model of broken clouds. However, this model cannot be directly incorporated into the radiation codes of current GCMs due to large time required to calculate the cloud radiative characteristics as functions of many parameters. To refine the GCM radiation codes, simple techniques for calculating the radiant flux in broken clouds must be developed, which would be sufficiently efficient and could adequately describe the stochastic geometry of cloud fields. The accuracy and applicability range of these techniques can be evaluated with the use of our numerical radiation model of broken clouds.

ACKNOWLEDGMENTS

The work was supported in part by DOE's ARM Program Contract No. 350114-A-Q1 as well as by the Russian Fund for Fundamental Research, Grant No. 95-05-14161.

REFERENCES

1. G.A. Titov, J. Atm. Sci. **47**, No. 1, 24–38 (1990).
2. V.E. Zuev, G.A. Titov, T.B. Zhuravleva, and S.Yu. Popov, in: *Proceedings of the Fourth ARM Science Team Meeting* (Charleston, South Carolina, 1994).
3. V.E. Zuev, G.A. Titov, T.B. Zhuravleva, and S.Yu. Popov, in: *Proceedings of the Fourth ARM Science Team Meeting* (Charleston, South Carolina, 1994).
4. V.E. Zuev and G.A. Titov, J. Atm. Sci. **51**, No. 2, 176–190 (1995).
5. G.A. Titov, T.B. Zhuravleva, and V.E. Zuev, submitted to J. Geophys. Res. (1995).
6. E.M. Feigel'son, ed., *Radiation in the Cloudy Atmosphere* (Gidrometeoizdat, Leningrad, 1981), 280 pp.
7. K.Ya. Kondrat'ev and V.I. Binenko, *Effect of Cloudiness on Radiation and Climate* (Gidrometeoizdat, Leningrad, 1984), 240 pp.
8. G.I. Marchuk, K.Ya. Kondrat'ev, V.V. Kozoderov, and V.I. Khvorost'yanov, *Clouds and Climate* (Gidrometeoizdat, Leningrad, 1986), 512 pp.
9. K.Ya. Kondrat'ev and L.B. Krasil'shchikov, eds., *High Precision Radiation Measurements in Meteorology* (Gidrometeoizdat, Leningrad, 1972), 512 pp.